

# REPORT DOCUMENTATION PAGE

Form Approved  
OMB No. 074-0188

Public reporting burden for this collection of information is estimated to average 1 hour per response, including the time for reviewing instructions, searching existing data sources, gathering and maintaining the data needed, and completing and reviewing this collection of information. Send comments regarding this burden estimate or any other aspect of this collection of information, including suggestions for reducing this burden to Washington Headquarters Services, Directorate for Information Operations and Reports, 1215 Jefferson Davis Highway, Suite 1204, Arlington, VA 22202-4302, and to the Office of Management and Budget, Paperwork Reduction Project (0704-0188), Washington, DC 20503

1. AGENCY USE ONLY (Leave blank)	2. REPORT DATE	3. REPORT TYPE AND DATES COVERED	
	1998	Proceedings	
4. TITLE AND SUBTITLE Spectroscopic Studies of Inhibited Opposed Flow Propane/Air Flames			5. FUNDING NUMBERS N/A
6. AUTHOR(S) R.R. Skaggs, R.G. Daniel, A.W. Mizolek, and K.L. McKesby			
7. PERFORMING ORGANIZATION NAME(S) AND ADDRESS(ES) U.S. Army Research Laboratory, Aberdeen Proving Ground, MD 21005			8. PERFORMING ORGANIZATION REPORT NUMBER N/A
9. SPONSORING / MONITORING AGENCY NAME(S) AND ADDRESS(ES) SERDP 901 North Stuart St. Suite 303 Arlington, VA 22203			10. SPONSORING / MONITORING AGENCY REPORT NUMBER N/A
11. SUPPLEMENTARY NOTES No copyright is asserted in the United States under Title 17, U.S. code. The U.S. Government has a royalty-free license to exercise all rights under the copyright claimed herein for Government purposes. All other rights are reserved by the copyright owner.			
12a. DISTRIBUTION / AVAILABILITY STATEMENT Approved for public release: distribution is unlimited.			12b. DISTRIBUTION CODE A
13. ABSTRACT (Maximum 200 Words) Planar Laser Induced Fluorescence (PLIF) is used to measure OH concentration profiles in an atmospheric pressure, opposed flow, propane ( $C_3H_8$ )/air flame. Flame inhibiting agents $CF_3Br$ , $N_2$ , $Fe(CO)_5$ , $C_3F_7H$ , $C_3F_6H_2$ , $CH_3P(O)(OCH_3)_2$ , and $P_3N_3F_6$ were added to the flame and relative OH concentration profiles were measured as each flame was extinguished. The OH profiles illustrate that addition of $N_2$ , $C_3F_6H_2$ , and $C_3F_7H_2$ , and $C_3F_7H$ , to the flame produced smaller changes in OH concentrations relative to $CF_3Br$ implying these agents have chemical inhibition capacities less than $CF_3Br$ . However, the addition of $CH_3P(O)(OCH_3)_2$ and $Fe(CO)_5$ to the flame demonstrated chemical inhibition capabilities greater than $CF_3Br$ with larger changes in OH concentrations.			
14. SUBJECT TERMS SERDP, SERDP Collection, spectroscopy, planar laser induced fluorescence, PLIF, flame			15. NUMBER OF PAGES 7
			16. PRICE CODE N/A
17. SECURITY CLASSIFICATION OF REPORT unclass	18. SECURITY CLASSIFICATION OF THIS PAGE unclass	19. SECURITY CLASSIFICATION OF ABSTRACT unclass	20. LIMITATION OF ABSTRACT UL

NSN 7540-01-280-5500

Standard Form 298 (Rev. 2-89)  
Prescribed by ANSI Std. Z39-18  
298-102

20000720 167

INTEC QUALITY ENGINEERING

## SPECTROSCOPIC STUDIES OF INHIBITED OPPOSED FLOW PROPANE/AIR FLAMES

R.R. SKAGGS, R.G. DANIEL, A.W. MIZIOLEK, AND K.L. MCNESBY

*U.S. Army Research Laboratory*

*Aberdeen Proving Ground, MD 21005*

### ABSTRACT

Planar Laser Induced Fluorescence (PLIF) is used to measure OH concentration profiles in an atmospheric pressure, opposed flow, propane ( $C_3H_8$ )/air flame. Flame inhibiting agents  $CF_3Br$ ,  $N_2$ ,  $Fe(CO)_5$ ,  $C_3F_7H$ ,  $C_3F_6H_2$ ,  $CH_3P(O)(OCH_3)_2$ , and  $P_3N_3F_6$  were added to the flame and relative OH concentration profiles were measured as each flame was extinguished. The OH profiles illustrate that addition of  $N_2$ ,  $C_3F_6H_2$ , and  $C_3F_7H$ , to the flame produced smaller changes in OH concentrations relative to  $CF_3Br$  implying these agents have chemical inhibition capacities less than  $CF_3Br$ . However, the addition of  $CH_3P(O)(OCH_3)_2$  and  $Fe(CO)_5$  to the flame demonstrated chemical inhibition capabilities greater than  $CF_3Br$  with larger changes in OH concentrations.

### INTRODUCTION

Fire protection on military platforms, including ground fighting vehicles, is being challenged by the impending loss of the ubiquitous fire fighting agent halon 1301 ( $CF_3Br$ ) due to environmental concerns related to the destruction of the stratospheric ozone layer. Replacement fire extinguishment agents need to be found that will satisfy numerous criteria including: fast fire suppression, minimum production of toxic gases when used, low toxicity, compatibility with storage materials and environmental friendliness.

The U.S. Army's search for halon replacement agents has largely involved an empirical approach of testing and evaluation of commercially available compounds/systems. An alternative approach is to study the fundamental physical and chemical mechanisms responsible for flame inhibition with the hope that such studies will uncover differences in the flame inhibition mechanisms which will lead to new chemicals for further consideration and testing. To this end, we have recently initiated planar laser induced fluorescence (PLIF) measurements of the OH radical species as flame extinction was approached in a non-premixed, atmospheric pressure, opposed flow propane/air flame inhibited by halon 1301 [ $CF_3Br$ ],  $N_2$ ,  $Fe(CO)_5$ , FM-200 [ $C_3F_7H$ ], FE-36 [ $C_3F_6H_2$ ], DMMP [ $CH_3P(O)(OCH_3)_2$ ], PN [ $P_3N_3F_6$ ]. Presented here are preliminary results from this study of compounds which represent distinctly different chemical families in order to understand the differences between each agent's inhibition mechanism.

### BACKGROUND

Chemical inhibition in a flame arises from the lowering of the radical concentrations due to scavenging reactions. In general, effective inhibition mechanisms contain two types of reactions: a) radical scavenging reactions, and b) reactions regenerating inhibitor species that participate in the inhibition cycle. As an example, for  $CF_3Br$  inhibition a free bromine from decomposed  $CF_3Br$  forms HBr which chemically reacts with a hydrogen atom and reduces the flame's hydrogen concentration. The consequence of hydrogen recombination is the overall available radical concentrations (H, O, OH) and the rate of chain-branching reactions are reduced [1,2,3,4] while regeneration of HBr and Br<sub>2</sub> occurs carrying on the inhibition cycle.

The chemicals  $Fe(CO)_5$ , DMMP, and PN investigated in our laboratory flame system were chosen based on a comprehensive evaluation [5] of fire inhibitors that are more effective than  $CF_3Br$ . The inhibition mechanisms for  $Fe(CO)_5$ , DMMP, and PN are believed to be generally similar to the HBr mechanism. For these postulated mechanisms, each agent decomposes during combustion into inhibition cycle scavenging species, e.g.  $FeO$ ,  $FeOH$ ,  $Fe(OH)_2$  for  $Fe(CO)_5$  addition, [6] and HOPO and HOPO<sub>2</sub> for DMMP and PN addition [7]. In the reaction zone of flames, these scavenging species proceed to behave much like HBr in scavenging hydrogen atoms. FM-200 and FE-36 were studied here due to their popularity as candidate halon replacement agents. FM-200 and FE-36 are refrigerants and it is assumed that their primary fire inhibition capabilities are due to their physical properties of high heat capacities with some chemical reactivity due to  $CF_3$  radical [8].

In order to understand a chemical's inhibition mechanism in terms of physical and/or chemical contributions, both  $N_2$  and  $CF_3Br$  are included in this study. That is,  $N_2$  represents the upper boundary for an agent's physical influence on flame inhibition since it has no chemical inhibition capabilities.  $CF_3Br$  which has been shown [9] that at least 20 % of its inhibition potential is caused by its physical properties offers a good intermediate point with which to compare and contrast the other agents studied.

## EXPERIMENTAL

OH PLIF imaging measurements were made using the arrangement presented in **Figure 1**. The opposed flow burner apparatus is located inside a stainless steel hood to contain any toxic fumes that are exhausted from the burner. All flames analyzed in this work were studied at atmospheric pressure and consisted of 7.0 L/min synthetic air (79%  $N_2$  + 21%  $O_2$ ) flowing from the lower duct, and 5.6 L/min of propane flowing from the upper duct. The oxidizer and fuel ducts are separated a distance of 1.2 cm and the duct diameter is 2.54 cm. Based on the flow conditions and duct separation, the luminous flame zone is located on the oxidizer side of the stagnation plane. For all studies presented here, the inhibitor agents are added to the oxidizer flow in gaseous form at room temperature with the exception of  $Fe(CO)_5$ , which was cooled to 11°C and DMMP which was heated to 70°C. Opposed flow burners have been used for some time to study the capabilities of an inhibitor agent because a global parameter, the extinction strain rate [10], can be determined which describes the flame's strength at extinction [11,12,13,14]. The extinction strain rate is useful because a decreased value demonstrates an inhibitor's efficiency. PLIF measurements of radical concentrations (O, H, OH) are complimentary to the extinction strain rate because the measurements illustrate an inhibitor's influence on the radical concentration profiles in the flame zone which indicates if the flame's radical chemistry is being perturbed by agent addition.

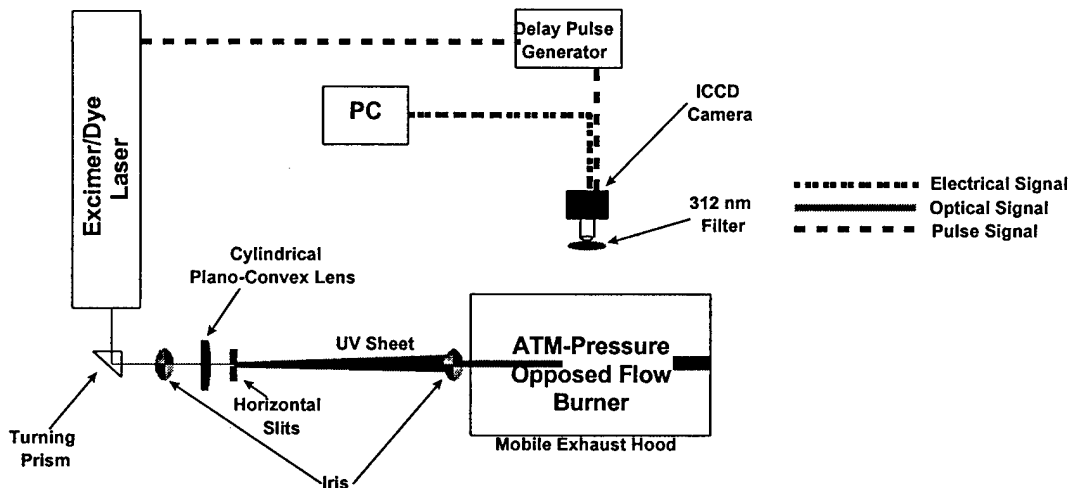


**Figure 1:** Schematic diagram of the experimental apparatus.

Planar laser induced fluorescence images were measured using a Lambda Physik excimer/dye laser system. This system consists of a Lambda Physik Compex 102 XeCl excimer laser, a Scanmate 2 dye laser (Coumarin 153) and a Second Harmonic Generator (SHG). The fundamental output of the dye laser (560 nm wavelength) was frequency doubled in the SHG unit with a BBO crystal to approximately 281 nm. The UV laser radiation was tuned to the peak of the  $R_2(9.5)$  transition at 281.8 nm ((1,0)  $A^2\Sigma^+ \leftarrow X^2\Pi$ ) [15,16,17]. The UV light output of the SHG unit enters an optical train where the beam is turned 90°, apertured by a sub mm iris, projected through a cylindrical plano convex lens to form the UV beam into a vertical sheet. To create a uniform sheet width, the sheet is apertured with 0.5 mm vertical slits as it is projected toward the center of the burner. The UV sheet is apertured just before the burner to produce a vertically uniform intensity that is 1.2 cm in height allowing passage through the entire burner flow field. Laser induced fluorescence from OH passes through a band pass filter centered at 312 nm with a 11 nm bandwidth and is detected with a Princeton Instruments ICCD camera (Model 120) coupled with a Nikon UV lens located at 90° with respect to the UV sheet. The ICCD camera, which has an active area of 384 x 576 pixels, has a

field of view with this optical arrangement of approximately  $33 \text{ cm}^2$  and each image recorded was acquired with 25 total accumulations on the camera.

## RESULTS

The effectiveness of a particular flame inhibitor is typically characterized by its influence on a flame's propagation chemistry. The most common indicators of the overall reaction rates for premixed and diffusion flame systems are the burning velocity and extinction strain rate respectively. For premixed flames, the addition of an inhibitor decreases the burning velocity. For diffusion flames, the addition of an inhibitor increases the characteristic chemical reaction time for the same flow time. That is, inhibitor concentration increases in a non-premixed flame can cause chemical reactions to proceed at times near the characteristic flow time which eventually can lead to flame extinction. For premixed and non-premixed systems, measurements of radical concentrations ( $\text{O}$ ,  $\text{H}$ ,  $\text{OH}$ ) serve as useful indicators of the chemistry being affected by inhibitor addition and are complimentary to burning velocity and extinction strain rate measurements.  $\text{OH}$  is monitored in the flames studied here because it is relatively simple to measure and it is a good indicator of the overall radical pool concentration, even though  $\text{H}$ ,  $\text{O}$ , and  $\text{OH}$  have been found to not be fully equilibrated in diffusion flames [18].

Figure 2 presents two representative two-dimensional images of  $\text{OH}$  fluorescence for an uninhibited propane/air flame and for a propane/air flame to which  $\text{CF}_3\text{Br}$  was added (1.5 % by volume). Both images, which are uncorrected for laser energy fluctuations and local quenching rates, illustrate the presence of two luminous zones as the UV sheet passes through the flame. The lower, thicker zone is the fluorescence from the  $\text{OH}$  transition while the upper, thinner zone is the broadband fluorescence due to derivative fuel species such as polycyclic aromatic hydrocarbons. To construct a spatially resolved  $\text{OH}$  LIF profile from a  $\text{OH}$  PLIF image, as shown on the right hand side of Figure 2, the pixel intensity corresponding to a given height between the fuel and oxidizer ducts (spatial resolution approximately 0.149 mm/pixel) was summed and averaged over a 1 mm horizontal width. The two-dimensional images and LIF profiles illustrate that addition of  $\text{CF}_3\text{Br}$  to the propane flame causes a decrease in the  $\text{OH}$  fluorescence signal while the broadband fluorescence appears to increase just slightly. Similar results have been seen previously for  $\text{CF}_3\text{Br}$  addition to hydrocarbon diffusion flames [19,20].

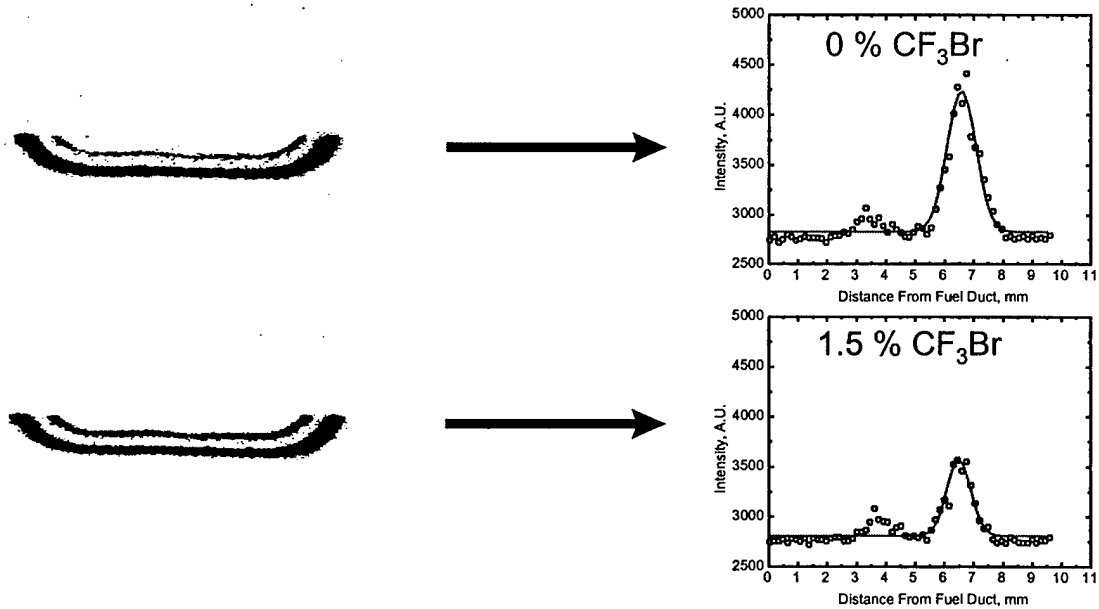
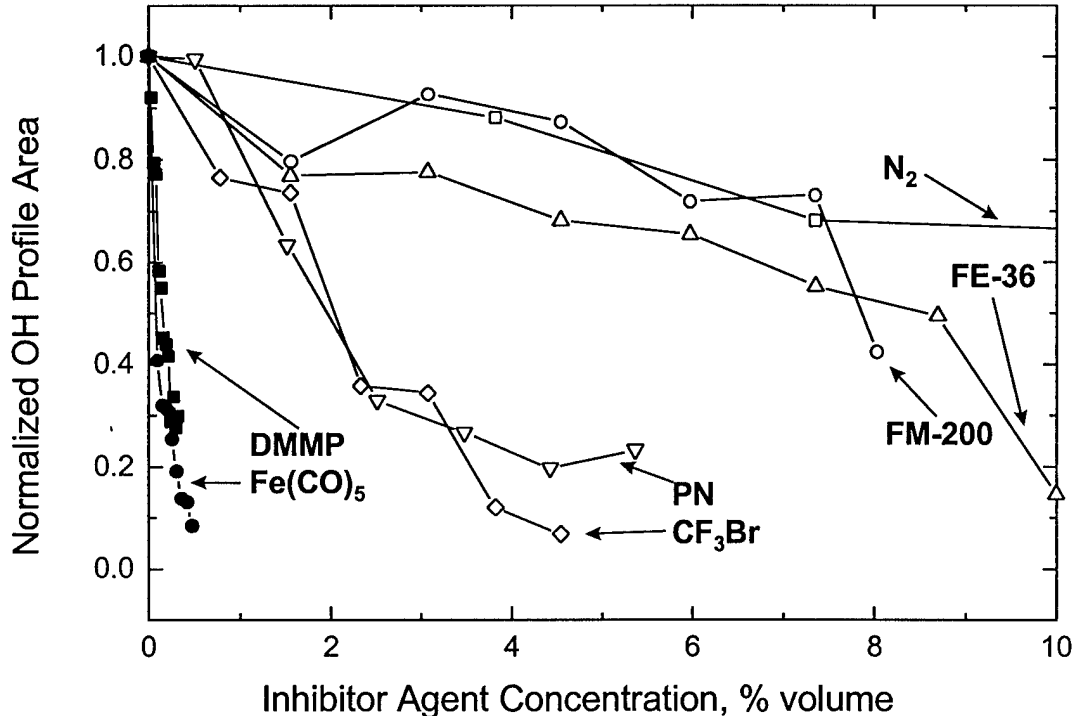


Figure 2: Representative PLIF images and the corresponding  $\text{OH}$  intensity profiles from an opposed flow propane/air flame seeded with 0 % (by volume)  $\text{CF}_3\text{Br}$  and 1.5 % (by volume)  $\text{CF}_3\text{Br}$ . Note the orientation of the PLIF images with respect to the burner system places the fuel and air ducts at the top and bottom of each image respectively.

Obviously the addition of an inhibitor to a flame gives rise to modifications in the flame structure. Specifically, addition of an inhibitor can change the position and width of the flame's reaction zone. Previous studies have shown [21,22,23,24,25] that a decrease in the flame's reaction zone width indicates increased localized strain, which can cause local quenching or flame extinction [26]. The width of the flame's reaction zone may be characterized by the width of a radical profile [21]. For the analysis of reaction zone modifications and relative OH concentrations, each OH intensity profile is fit to a gaussian function. A gaussian function determines the area under the profile curve which provides a general indicator of the entire OH profile for a given flame condition. Figure 3 plots the results of the measured OH profile areas versus each inhibitor agent's concentration as the flames were stepped towards extinction.



**Figure 3:** Normalized OH LIF profile areas versus agent delivery concentrations. The (○) are the  $N_2$  data, the (◊) are the FM-200 data, the (+) are the FE-36 data, the (△) are the PN data, the (○) are the  $CF_3Br$  data, the (■) is the DMMP data and the (●) are the  $Fe(CO)_5$ .

The reported OH profile areas are averaged over three or more separate inhibitor extinction experiments, where the data for each experiment are normalized to the OH profile area measured in the uninhibited flame acquired prior to each inhibitor extinction experiment to account for changes in burner and camera conditions. The data here indicate that there are both physical and chemical modes of inhibition being observed for the agents studied.  $N_2$  has the least impact on OH with respect to the other agents studied and for the concentration range plotted in Figure 3 the flame was not even extinguished by  $N_2$ . Similar results are observed for the two fluorinated propanes (FM-200 and FE-36) which show initially small declines in OH, but more rapid decreases as extinction is approached. For the other agents studied (PN,  $CF_3Br$ , DMMP, and  $Fe(CO)_5$ ), the addition of these inhibitors show more dramatic decreases in the measured OH values. Table I lists the observed inhibitor concentrations in the air stream at extinction for each agent studied here and their estimated uncertainties.

**Table I:** Inhibitor concentrations (% volume) and uncertainty ( $\pm$  % volume) at flame extinction

Inhibitor Agent	$N_2$	FE-36	FM-200	PN	$CF_3Br$	$Fe(CO)_5$	DMMP
Extinction Concentration	35.9	10.64	9.1	6	4.4	0.5	0.4
Estimated Uncertainty	12.3	1.56	1.88	0.63	1.47	0.10	0.03

It should be noted that the extinction concentration for  $\text{CF}_3\text{Br}$  is very similar to values found for analogous flames and cup burners [20], while the fluorinated propanes are slightly higher than their reported cup burner values [27]. Unfortunately there are no cup burner values reported for DMMP. Recent cup burner experiments for PN [28] indicate the value observed in our experiments is a factor of 6 greater than the literature value. At this time there is no explanation for the PN extinction concentration discrepancy and future experiments will address this issue in more detail.

**Figure 4** presents a plot of the strain rates ( $\text{sec}^{-1}$ ) calculated using the Seshadri and Williams expression [10] versus the measured OH Full Width Half Maximum (FWHM, mm) values for a series of uninhibited propane air flames with proportional increases in air and fuel flow rates. The width of the flame's reaction zone is defined here as the distance of one half of the maximum intensity of the gaussian OH profile. Previous studies [23] have denoted the width of a laminar flame reaction zone using one half of the maximum value of a temperature profile. Interestingly the data in **Figure 4** imply a relationship between the OH profile width, i.e. reaction zone width, and the strain rate with the OH profile width decreasing as the strain rate increases. To quantify the relationship between the OH profile width and strain rate, the data in **Figure 4** were fit to a second order decay function to develop an analytical function. Using the developed analytical equation, changes in OH profile widths can be used to indicate what strain rate the flame is experiencing as each inhibitor agent is added to the flame.

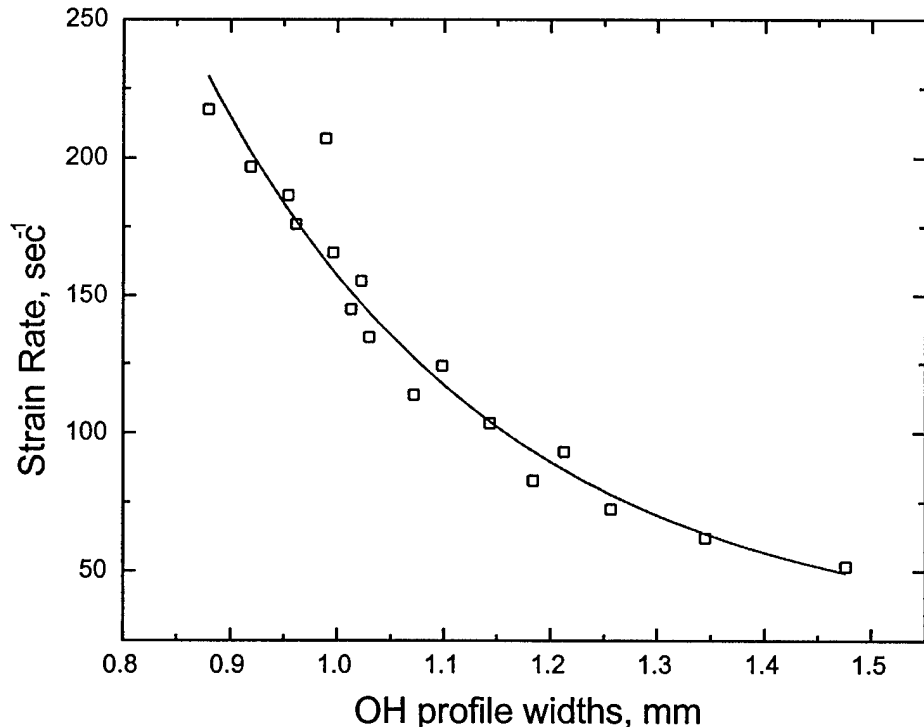


**Figure 4:** Calculated propane/air strain rates ( $\text{sec}^{-1}$ ) versus measured OH profile widths (FWHM, mm). The ( ) symbols are the averaged measured profile values while the solid line directly beneath is a second order exponential decay fit to the data.

**Table II** lists measured OH profile widths and corresponding strain rates at selected agent concentrations for the uninhibited flame and each inhibited flame. Beside  $\text{N}_2$ , the selected inhibitor concentrations are slightly less than the concentrations required for flame extinction and were chosen because the gaussian fitted width values have uncertainty values less than 5 %. It should be noted that the strain rate value listed in **Table II** for the uninhibited flame is slightly lower than the calculated [10] value of  $72.51 \text{ sec}^{-1}$ . The strain rate value listed in **Table II** is determined using the average OH profile width acquired from each OH profile that was measured in the uninhibited flame prior to each inhibitor extinction experiment and in two flame strain rate experiments. The uncertainty due to measurement variance with the average uninhibited OH width value is 11 %.

The Table II width values indicate that the agents, N<sub>2</sub>, FE-36, FM-200 do not possess width changes significantly different than the uninhibited flame. On the contrary CF<sub>3</sub>Br, PN, DMMP, and Fe(CO)<sub>5</sub> exhibit width changes that are equal to or greater than a 20 % decrease from the uninhibited width value. These width decreases correspond to strain rate values that are at least double the uninhibited flame value. From the strain rate data listed in Table II, the inhibitor agents are ranked from lowest to highest strain rate values as: N<sub>2</sub>, FE-36, FM-200 having the lowest strain rate values followed, in increasing strain rate values, by CF<sub>3</sub>Br < PN < DMMP < Fe(CO)<sub>5</sub>. The strain rate data trends imply that inhibitor agents with more physical suppression capabilities exhibit less effect on the flame structure and strain rate than inhibitors with enhanced chemical suppression capabilities.

*Table II: Measured OH profile widths (FWHM, mm) and corresponding strain rates (sec<sup>-1</sup>) at selected inhibitor concentrations (% volume).*

	Inhibitor % Volume	OH profile width, mm	Strain Rate, sec <sup>-1</sup>
Uninhibited	0	1.30	70.50
N <sub>2</sub>	10.64	1.26	76.98
CF <sub>3</sub> Br	4.18	1.01	155.31
FE-36	8.68	1.27	74.69
FM-200	4.55	1.26	76.80
Fe(CO) <sub>5</sub>	0.48	0.76	342.44
PN	5.36	0.95	186.43
DMMP	0.20	0.81	292.21

## CONCLUSIONS

The results presented here show for the first time changes in OH profiles as extinction is approached in a series of inhibited atmospheric pressure, non-premixed, propane/air flames. The OH profiles from these flames illustrate that N<sub>2</sub>, FE-36, and FM-200, with smaller changes in OH areas relative to CF<sub>3</sub>Br, exhibit chemical inhibition capacities less than CF<sub>3</sub>Br. On the contrary, DMMP and Fe(CO)<sub>5</sub> demonstrate chemical inhibition capabilities greater than CF<sub>3</sub>Br with their larger changes in OH. For the inhibitors studied, agent concentrations at extinction support these observations with a CF<sub>3</sub>Br concentration of 4.4 % (by volume) compared to N<sub>2</sub> with a concentration of 35.9 % and DMMP and Fe(CO)<sub>5</sub> each having concentrations less than 1 %. Analysis of the OH profile widths and their correlation to the flame's strain rate indicate that as the OH profile widths decrease the strain rates increase. For flames inhibited by Fe(CO)<sub>5</sub>, DMMP, and PN, the OH profiles width and strain rate changes are greater than those experienced in the CF<sub>3</sub>Br inhibited flame. Contrariwise, flames inhibited by N<sub>2</sub>, FM-200, and FE-36 do not demonstrate profile width and strain rate changes much different than those observed for the uninhibited flame.

## ACKNOWLEDGMENTS

The authors would like to thank Anthony Hamins (NIST) for burner fabrication and Valeri Babushok (NIST) for insightful suggestions and comments concerning experiments and results. This work was supported by the Next Generation Fire Suppression Technology Program under the auspices of the U.S. Army TACOM (Steve McCormick). Finally R. Skaggs would like to acknowledge financial support from the Army Research Laboratory through an American Society for Engineering Education Postdoctoral Fellowship.

## REFERENCES

1. Dixon-Lewis, G., Simpson, R.J., *Sixteenth Symposium (International) on Combustion*, The Combustion Institute, Pittsburgh, 1976, p.1111.
2. Westbrook, C.K. *Combust. Sci. Technol.* 23: 191 (1980).
3. Westbrook, C.K. *Nineteenth Symposium (International) on Combustion*, The Combustion Institute, Pittsburgh, 1982, p.127.
4. Westbrook, C.K. *Combust. Sci. Technol.* 34: 201 (1983).
5. Babushok, V., Tsang, W. *Chemical and Physical Processes in Combustion: Proceedings of Fall Technical Meeting of the Eastern States Section of the Combustion Institute*, 1997, p.79.
6. Rumminger, M.D., Reinelt, D., Babushok, V.I., and Linteris, G.T., *Combust. Flame* 116: 207 (1999).
7. MacDonald, M.A. Jayaweera, T.M. Fisher, E.M., Gouldin, F.C. *Combust. Flame* 116: 166 (1999).
8. Williams, B.A., Fleming, J.W., and Sheinson, R.S., *Halon Options Technical Working Conference*, Albuquerque, 1997, p.31.
9. Noto, T., Babushok, V., Burgess, D.R., Hamins, A., Tsang, W., Mizolek, A., *Twenty-Sixth Symposium (International) on Combustion*, Pittsburgh 1996, p.1377.
10. Seshadri, K. and Williams, F., *Int. J. Heat and Mass Transfer* 21:251 (1978).
11. Potter, A.E., Heimel, S., and Butler, J.N., *Eighth Symposium (International) on Combustion*, The Combustion Institute, Pittsburgh, 1962, p.1027.
12. Carrier, G.F., Fendell, F.E., and Marble, F.E., *SIAM J. Appl Math.* 28: 463-500 (1975)
13. Linan, A. *Acta Astronaut* 1: 1007 (1974).
14. Williams, F.A. *Fire Saf. J.* 3:163 (1981)
15. Chidsey, I.L., and Crosley, D.R., *J. Quant. Spectrosc. Radiat. Transf.* 23: 187 (1980)
16. Dieke, G.H., and Croswright, H.M., *J. Quant. Spectrosc. Radiat. Transf.* 2: 97 (1962).
17. Kotlar, A., Private Communication (1998).
18. Smyth, K.C., Tjossem, P.J.H., Hamins, A., and Miller, J.H., *Combust. Flame* 79: 366 (1990).
19. Masri, A.R., Dally, B.B., Barlow, R.S., and Carter, C.D., *Combust. Sci. Technol.* 113-114: 17 (1996).
20. Smyth, K.C., and Everest, D., *Twenty-Sixth Symposium (International) on Combustion*, The Combustion Institute, Pittsburgh, 1996, p.1385.
21. Peters, N. *Combust. Sci. Technol.* 30: 1 (1983).
22. Liew, S.K., Bray, K.N.C., and Moss, J.B., *Combust. Flame* 56: 199 (1984).
23. Haworth, D.C., Drake, M.C., and Blint, R.J., *Combust. Sci. Technol.* 60: 287 (1988).
24. Roberts, Wm. L., Driscoll, J.F., Drake, M.C., and Ratcliffe, J.W., *Twenty-Fourth Symposium (International) on Combustion*, The Combustion Institute, Pittsburgh, 1992, p.169.
25. Miller, J.H., *Chemical and Physical Processes in Combustion: Proceedings of Fall Technical Meeting of the Eastern States Section of the Combustion Institute*, 1996, p.1.
26. Bilger, R.W. *Twenty-Second Symposium (International) on Combustion*, The Combustion Institute, Pittsburgh 1996, p.1377.
27. *Cup-Burner Flame Extinguishment Concentrations*, NMERI Report <http://www.nmeri.unm-cget>, (1998).
28. Kaizerman, J.A., and Tapscott, R.E. *Advanced Streaming Agent Development, Volume III: Phosphorus Compounds*, New Mexico Engineering Research Institute, Report No. NMERI 96/5/32540, (1996).